JOURNAL OF MATERIALS PROCESSING TECHNOLOGY 199 (2008) 457–458

available at www.sciencedirect.com

ScienceDirect

journal homepage: www.elsevier.com/locate/jmatprotec

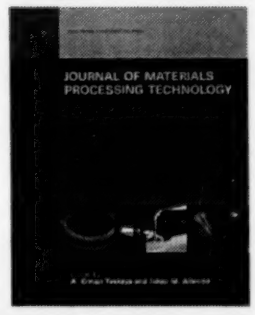

Author Index of Volume 199

Abbasi, M.H., 10
Adda-bedia, E.A., 199
Ahmad, R., 363
Ahmadabadi, M.N., 304
Ahzi, S., 74
Al Omar, A., 140
Ali, A.A., 193
Allen, S.J., 102
Al-Qureshi, H.A., 417
Alves, M.C., 417
An, L., 56
Angamuthu, K., 185
Aniolek, M., 84
Anwar, U.M.K., 156
As, N., 119
Atsumi, S.-Y., 163

Barreiros, F.M., 425
Belnou, F., 150
Benzair, A., 199
Bernard, J., 150
Bierwagen, G.P., 321
Blum, H., 341
Bogicevic, C., 314
Bouaziz, Z., 402
Bouazza, M., 199
Brandão, L.C., 234
Brinkman, A.W., 412

Çakır, O., 337
Chayoukhi, S., 402
Chen, F., 37
Chen, J.T., 456
Chen, L., 221
Chen, X., 256
Chenaoui, A., 140
Coelho, R.T., 234
Correia, J.P.M., 74
Crespo, A.C., 265

Dammak, H., 314
Dar, N.U., 379
Daridon, L., 74
de Abreu, H.F.G., 391
Dennis, R.S., 245
Dkiouak, R., 140
Dundar, T., 119
Duszczyk, J., 91

Ebrahimi, H., 287
Ebrahimi, R., 214

El Hassani, F.B., 140
Elbakkali, L., 140
El-Midany, A.A., 279
Ergun, C., 178

Fadaei Tehrani, A., 369
Fang, G., 91
Farias, J.P., 452
Francis, A.A., 279
Fu, H., 274

Gan, K., 173
García, H.P., 431
García, J.P., 431
Gotoh, M., 163
Gu, M., 173
Güllü, C., 448

Haddad, M.J., 369
Hamdan, H., 156
Haussonne, J.-M., 150
He, X., 27
Hiziroglu, S., 156, 440, 448
Hotza, D., 417
Houivet, D., 150
Hu, H., 256
Husson, C., 74

Idoipe, A.V., 431
Iqbal, A., 379

Jia, Y., 56

Kanaani, M., 214
Kanayama, K., 396
Karolak, F., 314
Kasprzak, W., 84
Kazeminezhad, M., 230
Kermanpur, A., 295
Khan, I., 379
Kılıç, M., 448
Kina, A.Y., 391
Klein, A.N., 417
Kolukisa, S., 437
Korkut, S., 119
Kurita, H., 84

Lei, S., 445
Levine, K.L., 321
Li, X., 221

Liang, L., 379

Ma, Y., 49
Maachou, M., 199
Mahdavian, S.M., 102
M'Saoubi, R., 64
Matías, J.C.H., 431
Miki, T., 396
Moosavi Nezhad, S.M., 124
Moshksar, M.M., 214
Murtaza, G., 363

Ning, H., 379

Okçu, O., 1
Outeiro, J.C., 64
Özçifçi, A., 1
Ozerdem, M.S., 437

Pandiyaraj, K.N., 130
Parlak, M., 412
Parsa, M.H., 304
Parvizian, J., 287
Pearson, I., 27
Pérez, M.R., 265
Poorganji, B., 304
Pournia, P., 304
Poursina, M., 287

Qayyum, A., 363

Rabinovitch, Y., 314
Ragab, A.R., 206
Rao, K.P., 185
Reese, S., 341
Reihanian, M., 214
Ren, L., 221
Rizzuti, S., 64
Rodrigues, A.R., 234
Ruan, X., 49

Sajjadi, S.A., 124
Saleem, M., 363
Santos, A.D., 327
Sarıdemir, M., 108
Schmidt, R., 412
Schwarze, M., 341
Scotti, A., 265
Selvarajan, V., 130
Sezgin, Z., 448
Shah, M.S., 363

Elsevier B.V.
doi:10.1016/S0924-0136(07)01443-4

Shamanian, M., 295
Shan, H., 221
Shen, Q., 37
Shirazi, H., 304
Shivpuri, R., 64
Silva, C.C., 452
Soares, M.R.F., 417
Sokolowski, J.H., 84
Soleimani Dorcheh, A., 10
Souza, J.A., 391
Souza, V.M., 391
Srinivasan, P.B., 185
Stiemer, M., 341
Sugimoto, H., 396
Sun, N., 221
Sun, S., 56
Sun, Z., 256, 445
Svendsen, B., 341

Tahir, P.M., 156
Takeuchi, K., 396
Tallman, D.E., 321
Tavares, S.S.M., 391
Teixeira, P., 327
Tétard, D., 314
Tian, Y., 41
Topçu, I.B., 108
Tounsi, A., 199
Tu, J.F., 245

Umbrello, D., 64
Unger, J., 341
Unsal, O., 119
Usta, M., 440
Ustaomer, D., 440

Vieira, M.T., 425

Wang, B., 49
Wang, C., 41
Wang, J., 274
Wu, L., 56

Xie, Y., 49

Yamagata, H., 84
Yamashita, M., 163
Yeganeh, V.E., 295
Young, K., 27
Yu, H., 49
Yu, L., 37
Yuying, Y., 445

Zakaullah, M., 363
Zebarjad, S.M., 124
Zehtab Yazdi, A., 124
Zghal, A., 402
Zhang, G., 56
Zhang, H.W., 456
Zhang, L., 37
Zhang, M., 274
Zhang, Z., 456
Zhao, G., 56
Zhou, H., 221
Zhou, J., 91
Zhou, Y., 41
Zhu, D., 41

JOURNAL OF MATERIALS PROCESSING TECHNOLOGY 199 (2008) 459–465

available at www.sciencedirect.com

ScienceDirect

journal homepage: www.elsevier.com/locate/jmatprotec

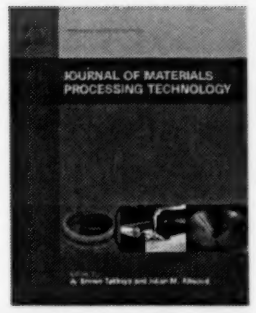

Subject Index of Volume 199

Activated anionic polymerization
Numerical simulation of reactive extrusion processes for activated anionic polymerization, 56
Adhesion
Study on adhesion resistance behavior of sample with striated non-smooth surface by laser processing technique, 221
AISI D3 tool steel
Material removal rate (MRR) study in the cylindrical wire electrical discharge turning (CWEDT) process, 369
Al alloy structure
Finite element modeling of electron beam welding of a large complex Al alloy structure by parallel computations, 41
Al–20% Si alloy
Thermal and metallographic characteristics of the Al–20% Si high-pressure die-casting alloy for monolithic cylinder blocks, 84
Aluminium
Effect of pocket design on metal flow through single-bearing extrusion dies to produce a thin-walled aluminium profile, 91
Chemical etching of aluminium, 337
Aluminium alloys
Mott–Schottky analysis of aluminium oxide formed in the presence of different mediators on the surface of aluminium alloy 2024-T3, 321
Analysis of variance (ANOVA)
An assessment of the carbothermic reduction of ilmenite ore by statistical design, 279
Angle-ply laminates
Prediction of stiffness degradation in hygrothermal aged $[\theta_m/90_n]_S$ composite laminates with transverse cracking, 199
Anodization
Mott–Schottky analysis of aluminium oxide formed in the presence of different mediators on the surface of aluminium alloy 2024-T3, 321
ANOVA
Material removal rate (MRR) study in the cylindrical wire electrical discharge turning (CWEDT) process, 369
Artificial Neural Network
Prediction of rubberized mortar properties using artificial neural network and fuzzy logic, 108
Artificial Neural Network approach to predict mechanical properties of hot rolled, nonresulfurized, AISI 10xx series carbon steel bars, 437
Attribute patterns
Automatic generation of a bill of materials based on attribute patterns with variant specifications in a customer-oriented environment, 431
Austenitic stainless steel
Influence of heat treatments on the intergranular corrosion resistance of the AISI 347 cast and weld metal for high temperature services, 391

Bead-over-bead technique
Fracture toughness of electron beam welded Ti6Al4V, 185
Beech
The effect of boiling time on the surface roughness of rotary-cut veneers from oriental beech (*Fagus orientalis* L.), 119
Influence of steaming on surface roughness of beech and sapele flooring material, 448
Bill of materials (BOM)
Automatic generation of a bill of materials based on attribute patterns with variant specifications in a customer-oriented environment, 431
Billet
Mathematical modeling of mould temperature field during continuous casting of steel, 49
Biomaterials
Synthesis and characterization of machinable calcium phosphate/lanthanum phosphate composites, 178
Biomimetics
Study on adhesion resistance behavior of sample with striated non-smooth surface by laser processing technique, 221
Blanking
Finite elements simulations of thin copper sheets blanking: Study of blanking parameters on sheared edge quality, 74
Boiling time
The effect of boiling time on the surface roughness of rotary-cut veneers from oriental beech (*Fagus orientalis* L.), 119
Borax
Impacts of some chemicals on combustion properties of impregnated laminated veneer lumber (LVL), 1
Boron compounds
Effect of boron treatment on surface characteristics of medium density fiberboard (MDF), 440

Calcination
Structural phase evolution with temperature of non-conventional particles in PIM, 425
Carbothermic reduction
An assessment of the carbothermic reduction of ilmenite ore by statistical design, 279
Characterization
Silica aerogel; synthesis, properties and characterization, 10

Elsevier B.V.
doi:10.1016/S0924-0136(07)01444-6

Charpy impact
Fracture toughness of electron beam welded Ti6Al4V, 185
Chemical etching
Chemical etching of aluminium, 337
Coated electrodes
Operational behavior assesment of coated tubular electrodes for SMAW hardfacing, 265
Combustion
Impacts of some chemicals on combustion properties of impregnated laminated veneer lumber (LVL), 1
Composites
Synthesis and characterization of machinable calcium phosphate/lanthanum phosphate composites, 178
Compressibility
The compressibility of Cu/SiC_p powder prepared by high-energy ball milling, 173
Compressive strength
Prediction of rubberized mortar properties using artificial neural network and fuzzy logic, 108
Computational simulation
Numerical optimization of gating system parameters for a magnesium alloy casting with multiple performance characteristics, 256
Constitutive equations
Flow stress behavior of two stainless steels: An experimental–numerical investigation, 287
Continuous casting
Mathematical modeling of mould temperature field during continuous casting of steel, 49
Corrosion protection
Mott–Schottky analysis of aluminium oxide formed in the presence of different mediators on the surface of aluminium alloy 2024-T3, 321
Cost estimation
Cost estimation of joints preparation for GMAW welding process using feature model, 402
C_T function
Prediction of hardness at different points of Jominy specimen using quench factor analysis method, 124
Cu/SiC_p
The compressibility of Cu/SiC_p powder prepared by high-energy ball milling, 173
CWEDT
Material removal rate (MRR) study in the cylindrical wire electrical discharge turning (CWEDT) process, 369
Cylinder shallow shell
Experimental study on controlling technique of surface deflection, 445

3D modeling of electromagnetic forming
Strategies for 3D simulation of electromagnetic forming processes, 341
Damage
Finite elements simulations of thin copper sheets blanking: Study of blanking parameters on sheared edge quality, 74
Deep drawing
The effect of lubrication on die expansion during the deep drawing of axisymmetrical steel cups, 102
Depth of etch
Chemical etching of aluminium, 337
Die
Effect of pocket design on metal flow through single-bearing extrusion dies to produce a thin-walled aluminium profile, 91
Die expansion
The effect of lubrication on die expansion during the deep drawing of axisymmetrical steel cups, 102
DOE
Material removal rate (MRR) study in the cylindrical wire electrical discharge turning (CWEDT) process, 369
Ductile fracture
Prediction of fracture limit curves in sheet metals using a void growth and coalescence model, 206
Dynamic material model
Characterization of deformation stability of medium carbon microalloyed steel during hot forging using phenomenological and continuum criteria, 140

Electroceramics
Control of the thickness distribution of evaporated functional electroceramic NTC thermistor thin films, 412
Electromagnetic forming
Strategies for 3D simulation of electromagnetic forming processes, 341
Electromagnetic–inelastic coupling
Strategies for 3D simulation of electromagnetic forming processes, 341
Electron beam weld
Fracture toughness of electron beam welded Ti6Al4V, 185
Electron beam welding
Finite element modeling of electron beam welding of a large complex Al alloy structure by parallel computations, 41
Electron transfer mediation
Mott–Schottky analysis of aluminium oxide formed in the presence of different mediators on the surface of aluminium alloy 2024-T3, 321
Electro-spinning
New generation of super absorber nano-fibroses hybrid fabric by electro-spinning, 193
Environment-friendly
Material development from wood powder without adhesive by vapor steaming compaction process, 396
Experimental benchmarks
A study on experimental benchmarks and simulation results in sheet metal forming, 327
Extrusion
Effect of pocket design on metal flow through single-bearing extrusion dies to produce a thin-walled aluminium profile, 91

FE simulation
Effect of pocket design on metal flow through single-bearing extrusion dies to produce a thin-walled aluminium profile, 91
Feedstock
Structural phase evolution with temperature of non-conventional particles in PIM, 425
FEM
A study on the computation of the redundant deformation factor in wire drawing of austenitic 304 stainless steel, 230
Fiberboard
Effect of boron treatment on surface characteristics of medium density fiberboard (MDF), 440
Finite element analysis
Hardness-based flow stress for numerical simulation of hard machining AISI H13 tool steel, 64

Finite element method (FEM)
Mathematical modeling of mould temperature field during continuous casting of steel, 49
Three-dimensional thermal simulation and experimental investigation of GTAW circumferentially butt-welded Incoloy 800 pipes, 295
Strategies for 3D simulation of electromagnetic forming processes, 341
Finite element modelling
A study on experimental benchmarks and simulation results in sheet metal forming, 327
Finite element simulation
Self-pierce riveting for sheet materials: State of the art, 27
Finite elements
Finite elements simulations of thin copper sheets blanking: Study of blanking parameters on sheared edge quality, 74
Flexural strength
Prediction of rubberized mortar properties using artificial neural network and fuzzy logic, 108
Flow instabilities
Characterization of deformation stability of medium carbon microalloyed steel during hot forging using phenomenological and continuum criteria, 140
Forging
Evaluation of microstructure change and hot workability of high nickel high strength steel using wedge test, 304
Fraction solid
Thermal and metallographic characteristics of the Al–20% Si high-pressure die-casting alloy for monolithic cylinder blocks, 84
Fracture limit curves
Prediction of fracture limit curves in sheet metals using a void growth and coalescence model, 206
Fracture toughness
Fracture toughness of electron beam welded Ti6Al4V, 185
Freeze-drying
Freeze-dried nanometric neodymium-doped YAG powders for transparent ceramics, 314
Friction
An upper-bound analysis of the tube extrusion process, 214
FTIR
Non-thermal plasma treatment for hydrophilicity improvement of grey cotton fabrics, 130
Fuzzy logic
Prediction of rubberized mortar properties using artificial neural network and fuzzy logic, 108

Gating system
Numerical optimization of gating system parameters for a magnesium alloy casting with multiple performance characteristics, 256
Glow discharge
Langmuir probe characterization of nitrogen plasma for surface nitriding of AISI-4140 steel, 363
Green density
Analyses of the fundamental parameters of cold die compaction of powder metallurgy, 417
Grey cotton fabric
Non-thermal plasma treatment for hydrophilicity improvement of grey cotton fabrics, 130
GTAW process
Three-dimensional thermal simulation and experimental investigation of GTAW circumferentially butt-welded Incoloy 800 pipes, 295

Hard machining
Hardness-based flow stress for numerical simulation of hard machining AISI H13 tool steel, 64
Hardfacing
Operational behavior assesment of coated tubular electrodes for SMAW hardfacing, 265
Hardness
Prediction of hardness at different points of Jominy specimen using quench factor analysis method, 124
Heat conduction and convection
Experimental and theoretical study of workpiece temperature when end milling hardened steels using (TiAl)N-coated and PcBN-tipped tools, 234
Heat treatment
Development of a localized heat treatment system for shape memory alloy wires using an ytterbium fiber laser, 245
High nickel high strength steel
Evaluation of microstructure change and hot workability of high nickel high strength steel using wedge test, 304
High-energy ball milling
The compressibility of Cu/SiC_p powder prepared by high-energy ball milling, 173
High-pressure die-casting
Thermal and metallographic characteristics of the Al–20% Si high-pressure die-casting alloy for monolithic cylinder blocks, 84
High-speed cutting
Experimental and theoretical study of workpiece temperature when end milling hardened steels using (TiAl)N-coated and PcBN-tipped tools, 234
High-speed milling
Modeling the effects of cutting parameters in MQL-employed finish hard-milling process using D-optimal method, 379
Hot deformation
Flow stress behavior of two stainless steels: An experimental–numerical investigation, 287
Hot forming
Characterization of deformation stability of medium carbon microalloyed steel during hot forging using phenomenological and continuum criteria, 140
Hot isostatic pressing
Freeze-dried nanometric neodymium-doped YAG powders for transparent ceramics, 314
Hot workability
Evaluation of microstructure change and hot workability of high nickel high strength steel using wedge test, 304
Hot-pressing (HP)
Fabrication of TZ-3Y20A/Mo multilayer composites by particle sedimentation method, 37
Hybrid fabric
New generation of super absorber nano-fibroses hybrid fabric by electro-spinning, 193
Hydroxylapatite
Synthesis and characterization of machinable calcium phosphate/lanthanum phosphate composites, 178
Hygrothermal effect
Prediction of stiffness degradation in hygrothermal aged $[\theta_m/90_n]_S$ composite laminates with transverse cracking, 199

Ilmenite
An assessment of the carbothermic reduction of ilmenite ore by statistical design, 279

Impregnation
Impacts of some chemicals on combustion properties of impregnated laminated veneer lumber (LVL), 1
Inclination angle
Modeling the effects of cutting parameters in MQL-employed finish hard-milling process using D-optimal method, 379
Incoloy 800
Three-dimensional thermal simulation and experimental investigation of GTAW circumferentially butt-welded Incoloy 800 pipes, 295
Incremental forming
Numerical simulation of incremental forming of sheet metal, 163
Inorganic natural powder
Structural phase evolution with temperature of non-conventional particles in PIM, 425
Interfaces
Fabrication of TZ-3Y20A/Mo multilayer composites by particle sedimentation method, 37
Internal/wall friction
Analyses of the fundamental parameters of cold die compaction of powder metallurgy, 417

Joint formation
Self-pierce riveting for sheet materials: State of the art, 27
Jominy test
Prediction of hardness at different points of Jominy specimen using quench factor analysis method, 124

Keyhole
Finite element modeling of electron beam welding of a large complex Al alloy structure by parallel computations, 41
Kinetics
Numerical simulation of reactive extrusion processes for activated anionic polymerization, 56

Labour cost
Cost estimation of joints preparation for GMAW welding process using feature model, 402
Langmuir probe characterization
Langmuir probe characterization of nitrogen plasma for surface nitriding of AISI-4140 steel, 363
Lanthanum phosphate
Synthesis and characterization of machinable calcium phosphate/lanthanum phosphate composites, 178
Laser
Study on adhesion resistance behavior of sample with striated non-smooth surface by laser processing technique, 221
Development of a localized heat treatment system for shape memory alloy wires using an ytterbium fiber laser, 245
Localized heat treatment
Development of a localized heat treatment system for shape memory alloy wires using an ytterbium fiber laser, 245
Low rate electron-beam evaporation
Control of the thickness distribution of evaporated functional electroceramic NTC thermistor thin films, 412
Lubrication
The effect of lubrication on die expansion during the deep drawing of axisymmetrical steel cups, 102
LVL
Impacts of some chemicals on combustion properties of impregnated laminated veneer lumber (LVL), 1

Machinable ceramics
Synthesis and characterization of machinable calcium phosphate/lanthanum phosphate composites, 178
Magnesium casting
Numerical optimization of gating system parameters for a magnesium alloy casting with multiple performance characteristics, 256
Magnesium titanate
Synthesis of pure $MgTiO_3$ by optimizing mixing/grinding condition of MgO + TiO_2 powders, 150
Malaysian species
Evaluation of surface quality of some Malaysian species as function of outdoor exposure, 156
Material behavior
Hardness-based flow stress for numerical simulation of hard machining AISI H13 tool steel, 64
Material cost
Cost estimation of joints preparation for GMAW welding process using feature model, 402
Mechanical properties
Self-pierce riveting for sheet materials: State of the art, 27
Structural phase evolution with temperature of non-conventional particles in PIM, 425
Medium density fiberboard
Effect of boron treatment on surface characteristics of medium density fiberboard (MDF), 440
Metal flow
Effect of pocket design on metal flow through single-bearing extrusion dies to produce a thin-walled aluminium profile, 91
MgO
Synthesis of pure $MgTiO_3$ by optimizing mixing/grinding condition of MgO + TiO_2 powders, 150
$MgTiO_3$
Synthesis of pure $MgTiO_3$ by optimizing mixing/grinding condition of MgO + TiO_2 powders, 150
Microalloyed steel
Characterization of deformation stability of medium carbon microalloyed steel during hot forging using phenomenological and continuum criteria, 140
Milling
Synthesis of pure $MgTiO_3$ by optimizing mixing/grinding condition of MgO + TiO_2 powders, 150
Mixing
Synthesis of pure $MgTiO_3$ by optimizing mixing/grinding condition of MgO + TiO_2 powders, 150
Modelling and simulation
Three-dimensional thermal simulation and experimental investigation of GTAW circumferentially butt-welded Incoloy 800 pipes, 295
Molds and dies
Experimental and theoretical study of workpiece temperature when end milling hardened steels using (TiAl)N-coated and PcBN-tipped tools, 234
Mott–Schottky analysis
Mott–Schottky analysis of aluminium oxide formed in the presence of different mediators on the surface of aluminium alloy 2024-T3, 321
Mould
Mathematical modeling of mould temperature field during continuous casting of steel, 49
MRR
Material removal rate (MRR) study in the cylindrical wire electrical discharge turning (CWEDT) process, 369
Multifield problems
Strategies for 3D simulation of electromagnetic forming processes, 341

Multilayer composites
Fabrication of TZ-3Y20A/Mo multilayer composites by particle sedimentation method, 37

Nanocrystalline TiO_2
Preparation and photocatalytic activity of nano-crystalline TiO_2 with uniform shape and size, 274
Nano-fibers
New generation of super absorber nano-fibroses hybrid fabric by electro-spinning, 193
Nanostructure
Silica aerogel; synthesis, properties and characterization, 10
Non-smooth Surfaces
Study on adhesion resistance behavior of sample with striated non-smooth surface by laser processing technique, 221
Non-thermal plasma
Non-thermal plasma treatment for hydrophilicity improvement of grey cotton fabrics, 130
NTC Thermistors
Control of the thickness distribution of evaporated functional electroceramic NTC thermistor thin films, 412
Numerical simulation
Numerical simulation of incremental forming of sheet metal, 163
Flow stress behavior of two stainless steels: An experimental–numerical investigation, 287
Numerical validation
A study on experimental benchmarks and simulation results in sheet metal forming, 327

Optimization
Numerical optimization of gating system parameters for a magnesium alloy casting with multiple performance characteristics, 256
Modeling the effects of cutting parameters in MQL-employed finish hard-milling process using D-optimal method, 379
Optimum die angle
An upper-bound analysis of the tube extrusion process, 214
Outdoor exposure
Evaluation of surface quality of some Malaysian species as function of outdoor exposure, 156

Parallel calculation
Finite element modeling of electron beam welding of a large complex Al alloy structure by parallel computations, 41
Particle sedimentation
Fabrication of TZ-3Y20A/Mo multilayer composites by particle sedimentation method, 37
Petrochemical pipes
Three-dimensional thermal simulation and experimental investigation of GTAW circumferentially butt-welded Incoloy 800 pipes, 295
Phase transformations
Structural phase evolution with temperature of non-conventional particles in PIM, 425
Photodegradation
Preparation and photocatalytic activity of nanocrystalline TiO_2 with uniform shape and size, 274
Pipe
Non-uniformity of residual stress profiles in butt-welded pipes in manual arc welding, 452
Polymers
Study on adhesion resistance behavior of sample with striated non-smooth surface by laser processing technique, 221
Pore radius
Non-thermal plasma treatment for hydrophilicity improvement of grey cotton fabrics, 130
Porosity
Analyses of the fundamental parameters of cold die compaction of powder metallurgy, 417
Powder injection moulding
Structural phase evolution with temperature of non-conventional particles in PIM, 425
Powder metallurgy
Analyses of the fundamental parameters of cold die compaction of powder metallurgy, 417
Powder morphology
The compressibility of Cu/SiC_p powder prepared by high-energy ball milling, 173
Pre-deformation
Finite element modeling of electron beam welding of a large complex Al alloy structure by parallel computations, 41
Prediction of mechanical properties
Artificial Neural Network approach to predict mechanical properties of hot rolled, nonresulfurized, AISI 10xx series carbon steel bars, 437
Primary Si
Thermal and metallographic characteristics of the Al–20% Si high-pressure die-casting alloy for monolithic cylinder blocks, 84
Process monitoring
Self-pierce riveting for sheet materials: State of the art, 27
Process techniques
Experimental study on controlling technique of surface deflection, 445
Product structures
Automatic generation of a bill of materials based on attribute patterns with variant specifications in a customer-oriented environment, 431

Quadrangular pyramidal shell
Numerical simulation of incremental forming of sheet metal, 163
Quench factor analysis
Prediction of hardness at different points of Jominy specimen using quench factor analysis method, 124

Rapid quenching
Thermal and metallographic characteristics of the Al–20% Si high-pressure die-casting alloy for monolithic cylinder blocks, 84
Reactive extrusion
Numerical simulation of reactive extrusion processes for activated anionic polymerization, 56
Redundant deformation factor
A study on the computation of the redundant deformation factor in wire drawing of austenitic 304 stainless steel, 230
Reference experimental results
A study on experimental benchmarks and simulation results in sheet metal forming, 327
Residual stress
Non-uniformity of residual stress profiles in butt-welded pipes in manual arc welding, 452

RSM
Material removal rate (MRR) study in the cylindrical wire electrical discharge turning (CWEDT) process, 369

Sapele
Influence of steaming on surface roughness of beech and sapele flooring material, 448
Self-bonding
Material development from wood powder without adhesive by vapor steaming compaction process, 396
Self-pierce riveting
Self-pierce riveting for sheet materials: State of the art, 27
SEM
Non-thermal plasma treatment for hydrophilicity improvement of grey cotton fabrics, 130
Modeling the effects of cutting parameters in MQL-employed finish hard-milling process using D-optimal method, 379
Sensitization
Influence of heat treatments on the intergranular corrosion resistance of the AISI 347 cast and weld metal for high temperature services, 391
Shape factor
Analyses of the fundamental parameters of cold die compaction of powder metallurgy, 417
Shape memory alloy
Development of a localized heat treatment system for shape memory alloy wires using an ytterbium fiber laser, 245
Shape performance
Numerical simulation of incremental forming of sheet metal, 163
Shear bands
Prediction of fracture limit curves in sheet metals using a void growth and coalescence model, 206
Sheared edge
Finite elements simulations of thin copper sheets blanking: Study of blanking parameters on sheared edge quality, 74
Sheet forming
Numerical simulation of incremental forming of sheet metal, 163
Sheet material
Self-pierce riveting for sheet materials: State of the art, 27
Sheet metal forming
A study on experimental benchmarks and simulation results in sheet metal forming, 327
Silica aerogel
Silica aerogel; synthesis, properties and characterization, 10
Simulation
Numerical simulation of reactive extrusion processes for activated anionic polymerization, 56
Prediction of hardness at different points of Jominy specimen using quench factor analysis method, 124
Sintering
Freeze-dried nanometric neodymium-doped YAG powders for transparent ceramics, 314
Stabilization
Influence of heat treatments on the intergranular corrosion resistance of the AISI 347 cast and weld metal for high temperature services, 391
Stainless steel surface nitriding
Langmuir probe characterization of nitrogen plasma for surface nitriding of AISI-4140 steel, 363
Statistical design
An assessment of the carbothermic reduction of ilmenite ore by statistical design, 279
Steaming
Influence of steaming on surface roughness of beech and sapele flooring material, 448
Stiffness reduction
Prediction of stiffness degradation in hygrothermal aged $[\theta_m/90_n]_S$ composite laminates with transverse cracking, 199
Stress perturbation function
Prediction of stiffness degradation in hygrothermal aged $[\theta_m/90_n]_S$ composite laminates with transverse cracking, 199
Substitute for plastics
Material development from wood powder without adhesive by vapor steaming compaction process, 396
Super absorber
New generation of super absorber nano-fibroses hybrid fabric by electro-spinning, 193
Superposition method
A study on the computation of the redundant deformation factor in wire drawing of austenitic 304 stainless steel, 230
Surface deflection
Experimental study on controlling technique of surface deflection, 445
Surface energy
Non-thermal plasma treatment for hydrophilicity improvement of grey cotton fabrics, 130
Surface quality
Chemical etching of aluminium, 337
Surface roughness
The effect of boiling time on the surface roughness of rotary-cut veneers from oriental beech (*Fagus orientalis* L.), 119
Evaluation of surface quality of some Malaysian species as function of outdoor exposure, 156
Effect of boron treatment on surface characteristics of medium density fiberboard (MDF), 440
Influence of steaming on surface roughness of beech and sapele flooring material, 448
Synthesis
Silica aerogel; synthesis, properties and characterization, 10

Taguchi method
Numerical optimization of gating system parameters for a magnesium alloy casting with multiple performance characteristics, 256
Temperature field
Mathematical modeling of mould temperature field during continuous casting of steel, 49
Temperature measurements
Experimental and theoretical study of workpiece temperature when end milling hardened steels using (TiAl)N-coated and PcBN-tipped tools, 234
Thermal analysis
Thermal and metallographic characteristics of the Al–20% Si high-pressure die-casting alloy for monolithic cylinder blocks, 84
Thermocouple measurement
Three-dimensional thermal simulation and experimental investigation of GTAW circumferentially butt-welded Incoloy 800 pipes, 295

Thickness distribution
Control of the thickness distribution of evaporated functional electroceramic NTC thermistor thin films, 412
Ti6Al4V
Fracture toughness of electron beam welded Ti6Al4V, 185
TiO_2
Synthesis of pure $MgTiO_3$ by optimizing mixing/grinding condition of $MgO + TiO_2$ powders, 150
Tool life
Modeling the effects of cutting parameters in MQL-employed finish hard-milling process using D-optimal method, 379
Tool steel
Hardness-based flow stress for numerical simulation of hard machining AISI H13 tool steel, 64
Tooling
Effect of pocket design on metal flow through single-bearing extrusion dies to produce a thin-walled aluminium profile, 91
Transparent ceramic
Freeze-dried nanometric neodymium-doped YAG powders for transparent ceramics, 314
Transverse cracking
Prediction of stiffness degradation in hygrothermal aged $[\theta_m/90_n]_S$ composite laminates with transverse cracking, 199
Traveling tool
Numerical simulation of incremental forming of sheet metal, 163
Tricalcium phosphate
Synthesis and characterization of machinable calcium phosphate/lanthanum phosphate composites, 178
Tube extrusion
An upper-bound analysis of the tube extrusion process, 214
Tubular electrodes
Operational behavior assesment of coated tubular electrodes for SMAW hardfacing, 265

Upper bound method
A study on the computation of the redundant deformation factor in wire drawing of austenitic 304 stainless steel, 230
Upper-bound theory
An upper-bound analysis of the tube extrusion process, 214

Variant handling
Automatic generation of a bill of materials based on attribute patterns with variant specifications in a customer-oriented environment, 431
Veneer
The effect of boiling time on the surface roughness of rotary-cut veneers from oriental beech (*Fagus orientalis* L.), 119
Viscoplasticity
Finite elements simulations of thin copper sheets blanking: Study of blanking parameters on sheared edge quality, 74
Void growth
Prediction of fracture limit curves in sheet metals using a void growth and coalescence model, 206

Waste rubber
Prediction of rubberized mortar properties using artificial neural network and fuzzy logic, 108
Wedge test
Evaluation of microstructure change and hot workability of high nickel high strength steel using wedge test, 304
Welded structures
Cost estimation of joints preparation for GMAW welding process using feature model, 402
Welding
Operational behavior assesment of coated tubular electrodes for SMAW hardfacing, 265
Non-uniformity of residual stress profiles in butt-welded pipes in manual arc welding, 452
Wire EDM
Material removal rate (MRR) study in the cylindrical wire electrical discharge turning (CWEDT) process, 369
Wood powder
Material development from wood powder without adhesive by vapor steaming compaction process, 396
Work-hardening
Analyses of the fundamental parameters of cold die compaction of powder metallurgy, 417

10xx series steel bars
Artificial Neural Network approach to predict mechanical properties of hot rolled, nonresulfurized, AISI 10xx series carbon steel bars, 437

YAG
Freeze-dried nanometric neodymium-doped YAG powders for transparent ceramics, 314

Zinc chloride
Impacts of some chemicals on combustion properties of impregnated laminated veneer lumber (LVL), 1

ELSEVIER

Volume 199, Issues 1–3, 1 April 2008

Journal of
Materials
Processing
Technology

www.elsevier.com/locate/jmatprotec

Contents

Impacts of some chemicals on combustion properties of impregnated laminated veneer lumber (LVL) 1
A. Özçifçi, O. Okçu

Silica aerogel; synthesis, properties and characterization 10
A. Soleimani Dorcheh, M.H. Abbasi

Self-pierce riveting for sheet materials: State of the art 27
X. He, I. Pearson, K. Young

Fabrication of TZ-3Y20A/Mo multilayer composites by particle sedimentation method 37
F. Chen, L. Yu, Q. Shen, L. Zhang

Finite element modeling of electron beam welding of a large complex Al alloy structure by parallel computations 41
Y. Tian, C. Wang, D. Zhu, Y. Zhou

Mathematical modeling of mould temperature field during continuous casting of steel 49
Y. Xie, H. Yu, X. Ruan, B. Wang, Y. Ma

Numerical simulation of reactive extrusion processes for activated anionic polymerization 56
L. Wu, Y. Jia, S. Sun, G. Zhang, G. Zhao, L. An

Hardness-based flow stress for numerical simulation of hard machining AISI H13 tool steel 64
D. Umbrello, S. Rizzuti, J.C. Outeiro, R. Shivpuri, R. M'Saoubi

Finite elements simulations of thin copper sheets blanking: Study of blanking parameters on sheared edge quality 74
C. Husson, J.P.M. Correia, L. Daridon, S. Ahzi

Thermal and metallographic characteristics of the Al–20% Si high-pressure die-casting alloy for monolithic cylinder blocks 84
H. Yamagata, H. Kurita, M. Aniolek, W. Kasprzak, J.H. Sokolowski

Effect of pocket design on metal flow through single-bearing extrusion dies to produce a thin-walled aluminium profile 91
G. Fang, J. Zhou, J. Duszczyk

The effect of lubrication on die expansion during the deep drawing of axisymmetrical steel cups 102
S.J. Allen, S.M. Mahdavian

Prediction of rubberized mortar properties using artificial neural network and fuzzy logic 108
İ.B. Topçu, M. Sarıdemir

The effect of boiling time on the surface roughness of rotary-cut veneers from oriental beech (Fagus orientalis L.) 119
T. Dundar, N. As, S. Korkut, O. Unsal

Prediction of hardness at different points of Jominy specimen using quench factor analysis method 124
A. Zehtab Yazdi, S.A. Sajjadi, S.M. Zebarjad, S.M. Moosavi Nezhad

Non-thermal plasma treatment for hydrophilicity improvement of grey cotton fabrics 130
K.N. Pandiyaraj, V. Selvarajan

Characterization of deformation stability of medium carbon microalloyed steel during hot forging using phenomenological and continuum criteria 140
F.B. El Hassani, A. Chenaoui, R. Dkiouak, L. Elbakkali, A. Al Omar

(Contents continued on page I)

0924-0136(20080401)199:1/3;1-Q

6017

(Contents continued from OBC)

Synthesis of pure $MgTiO_3$ by optimizing mixing/grinding condition of $MgO + TiO_2$ powders 150
J. Bernard, F. Belnou, D. Houivet, J.-M. Haussonne

Evaluation of surface quality of some Malaysian species as function of outdoor exposure 156
S. Hiziroglu, U.M.K. Anwar, H. Hamdan, P.M. Tahir

Numerical simulation of incremental forming of sheet metal..... 163
M. Yamashita, M. Gotoh, S.-Y. Atsumi

The compressibility of Cu/SiC_p powder prepared by high-energy ball milling 173
K. Gan, M. Gu

Synthesis and characterization of machinable calcium phosphate/lanthanum phosphate composites 178
C. Ergun

Fracture toughness of electron beam welded Ti6Al4V..... 185
K.P. Rao, K. Angamuthu, P.B. Srinivasan

New generation of super absorber nano-fibroses hybrid fabric by electro-spinning 193
A.A. Ali

Prediction of stiffness degradation in hygrothermal aged $[\theta_m/90_n]_S$ composite laminates with transverse cracking..... 199
E.A. Adda-bedia, M. Bouazza, A. Tounsi, A. Benzair, M. Maachou

Prediction of fracture limit curves in sheet metals using a void growth and coalescence model 206
A.R. Ragab

An upper-bound analysis of the tube extrusion process..... 214
R. Ebrahimi, M. Reihanian, M. Kanaani, M.M. Moshksar

Study on adhesion resistance behavior of sample with striated non-smooth surface by laser processing technique..... 221
H. Shan, H. Zhou, N. Sun, L. Ren, L. Chen, X. Li

A study on the computation of the redundant deformation factor in wire drawing of austenitic 304 stainless steel 230
M. Kazeminezhad

Experimental and theoretical study of workpiece temperature when end milling hardened steels using (TiAl)N-coated and PcBN-tipped tools 234
L.C. Brandão, R.T. Coelho, A.R. Rodrigues

Development of a localized heat treatment system for shape memory alloy wires using an ytterbium fiber laser 245
R.S. Dennis, J.F. Tu

Numerical optimization of gating system parameters for a magnesium alloy casting with multiple performance characteristics..... 256
Z. Sun, H. Hu, X. Chen

Operational behavior assesment of coated tubular electrodes for SMAW hardfacing..... 265
A.C. Crespo, A. Scotti, M.R. Pérez

Preparation and photocatalytic activity of nanocrystalline TiO_2 with uniform shape and size 274
M. Zhang, J. Wang, H. Fu

An assessment of the carbothermic reduction of ilmenite ore by statistical design 279
A.A. Francis, A.A. El-Midany

Flow stress behavior of two stainless steels: An experimental–numerical investigation 287
M. Poursina, H. Ebrahimi, J. Parvizian

Three-dimensional thermal simulation and experimental investigation of GTAW circumferentially butt-welded Incoloy 800 pipes..... 295
A. Kermanpur, M. Shamanian, V.E. Yeganeh

Evaluation of microstructure change and hot workability of high nickel high strength steel using wedge test 304
M.H. Parsa, M.N. Ahmadabadi, H. Shirazi, B. Poorganji, P. Pournia

Freeze-dried nanometric neodymium-doped YAG powders for transparent ceramics 314
Y. Rabinovitch, C. Bogicevic, F. Karolak, D. Tétard, H. Dammak

Mott–Schottky analysis of aluminium oxide formed in the presence of different mediators on the surface of aluminium alloy 2024-T3 321
K.L. Levine, D.E. Tallman, G.P. Bierwagen

A study on experimental benchmarks and simulation results in sheet metal forming..... 327
A.D. Santos, P. Teixeira

Chemical etching of aluminium 337
O. Çakır

Strategies for 3D simulation of electromagnetic forming processes 341
J. Unger, M. Stiemer, M. Schwarze, B. Svendsen, H. Blum, S. Reese

Langmuir probe characterization of nitrogen plasma for surface nitriding of AISI-4140 steel 363
M.S. Shah, M. Saleem, R. Ahmad, M. Zakaullah, A. Qayyum, G. Murtaza

Material removal rate (MRR) study in the cylindrical wire electrical discharge turning (CWEDT) process... 369
M.J. Haddad, A. Fadaei Tehrani

Modeling the effects of cutting parameters in MQL-employed finish hard-milling process using D-optimal method..... 379
A. Iqbal, H. Ning, I. Khan, L. Liang, N.U. Dar

Influence of heat treatments on the intergranular corrosion resistance of the AISI 347 cast and weld metal for high temperature services 391
A.Y. Kina, V.M. Souza, S.S.M. Tavares, J.A. Souza, H.F.G. de Abreu

Material development from wood powder without adhesive by vapor steaming compaction process..... 396
T. Miki, K. Takeuchi, H. Sugimoto, K. Kanayama

Cost estimation of joints preparation for GMAW welding process using feature model 402
S. Chayoukhi, Z. Bouaziz, A. Zghal

Control of the thickness distribution of evaporated functional electroceramic NTC thermistor thin films... 412
R. Schmidt, M. Parlak, A.W. Brinkman

Analyses of the fundamental parameters of cold die compaction of powder metallurgy..... 417
H.A. Al-Qureshi, M.R.F. Soares, D. Hotza, M.C. Alves, A.N. Klein

Structural phase evolution with temperature of non-conventional particles in PIM 425
F.M. Barreiros, M.T. Vieira

Automatic generation of a bill of materials based on attribute patterns with variant specifications in a customer-oriented environment 431
J.C.H. Matías, H.P. García, J.P. García, A.V. Idoipe

Artificial Neural Network approach to predict mechanical properties of hot rolled, nonresulfurized, AISI 10xx series carbon steel bars 437
M.S. Ozerdem, S. Kolukisa

Effect of boron treatment on surface characteristics of medium density fiberboard (MDF) 440
D. Ustaomer, M. Usta, S. Hiziroglu

Experimental study on controlling technique of surface deflection 445
Z. Sun, Y. Yuying, S. Lei

Influence of steaming on surface roughness of beech and sapele flooring material 448
M. Kılıç, S. Hiziroglu, C. Güllü, Z. Sezgin

Non-uniformity of residual stress profiles in butt-welded pipes in manual arc welding 452
C.C. Silva, J.P. Farias

Corrigendum to "3D modeling of material flow in friction stir welding under different process parameters" [J. Mater. Process. Technol. 183 (2007) 62–70] 456
H.W. Zhang, Z. Zhang, J.T. Chen

Author index..... 457

Subject index 459